Sixth International Conference on Durability of Concrete Structures
18 - 20 July 2018
University of Leeds, Leeds, West Yorkshire, LS2 9JT, United Kingdom
Paper Number PSE08

Sustainable Concrete with Seawater and Corrosion Resistant Reinforcement: Results of Monitoring of Corrosion Behaviour

E. Redaelli, M. Carsana, F. Lollini, M. Gastaldi and F.T. Isfahani
Department of Chemistry, Materials and Chemical Engineering, Politecnico di Milano, Italy

ABSTRACT

The use of seawater for mixing concrete in reinforced concrete structures is prohibited, since it can promote steel corrosion. However, the use of seawater would contribute to decrease the environmental impact of concrete, in particular in those coastal regions of the world where potable water is a precious resource. The project SEACON-INFRAVATION between University of Miami and Politecnico di Milano, with various industrial partners, aims at investigating the use of seawater for the construction of sustainable and durable reinforced concrete structures and infrastructures. Within the project, that included a vast campaign of laboratory tests, two demo projects – one in Italy and one in the US – were designed and executed with the aim of testing the use of seawater on-site and allowing long-term monitoring of the durability behavior. In Italy, a reinforced concrete culvert was built next to A1 motorway, close to Piacenza. The culvert collects the waters coming from the roadway that, during winter season, is subjected to de-icing salts; in addition, it is unsheltered from the rain and exposed to wetting and drying cycles. The culvert is divided into six segments, and each segment is representative of a given scenario in terms of type of concrete and type of reinforcement. Besides a reference segment, with carbon steel and chloride-free concrete, other segments were built using seawater concrete in combination with corrosion resistant reinforcement. Three types of corrosion resistant reinforcement were considered: an austenitic grade of stainless steel (1.4311), a duplex grade of stainless steel (1.4362) and GFRP. A concrete made with partial replacement of coarse aggregate with recycled asphalt pavement (RAP) was also considered. The corrosion conditions of the metallic reinforcements are monitored by means of potential measurements. The electrical resistivity of concrete is also monitored, and the evolution of carbonation and chloride penetration are periodically analysed on concrete cores taken from the culvert. This note presents the results that have been obtained during more than one year of monitoring of the corrosion conditions of the various types of reinforcement embedded in seawater concrete and compares them with results obtained in the laboratory.

Keywords: chlorides, concrete, corrosion, seawater, stainless steel, GFRP.

1.0 INTRODUCTION

Chloride-induced corrosion is one of the main causes of reinforced concrete (RC) deterioration, and for this reason today seawater, as well as other chloride-contaminated materials, shall not be used for concrete mixing (Bertolini *et al.*, 2013). However, the consumption of freshwater in the concrete industry contributes to the environmental impact of concrete, that could be reduced (in particular in those coastal regions of the world where potable water is a precious resource) by allowing the use of seawater together with corrosion resistant reinforcement (Lollini *et al.*, 2016a; Lollini *et al.*, 2016b).

The project SEACON-INFRAVATION aims at investigating the use of seawater for the construction of sustainable and durable RC structures and infrastructures. Within the project, that included a vast campaign of laboratory tests, two demo projects – one in Italy and one in the US – were designed and executed with the aim of testing the use of seawater on-site and allowing long-term monitoring of the durability behaviour. In Italy, a RC culvert was built next to A1 motorway, using different types of concrete and reinforcement (Redaelli *et al.*, 2017). The culvert was built in November 2016. This note presents the results of the measurements that were carried out during more than one year of monitoring of various parameters related with the durability behaviour of the materials.

2.0 METHODOLOGY

The RC culvert is 30 m long and it is made of 6 individual segments, 5 m long each, indicated with letters *A*-*F* (Fig. 1). The slab is 0.8 m wide and 0.15 m thick and it is surrounded by two inclined lateral walls (non-reinforced). Each slab is reinforced with a mesh, made of bars with diameter of 16 mm and spacing of 200 mm. The design concrete cover is 30 mm. Each segment is representative of a combination of type of concrete and type of reinforcement, as shown in Table 1: segment *A* is

made with *reference* concrete (initially chloride-free) and carbon steel (CS) reinforcement; segments *B*, *C*, *D* and *E* are all made with *seawater* concrete (where seawater was used instead of freshwater) and CS, austenitic grade of stainless steel (1.4311 or SS-304), duplex grade of stainless steel (1.4362 or SS-23-04) and glass fibre reinforced polymer (GFRP) reinforcements, respectively; segment *F* is made with *RAP* concrete (where a fraction of coarse aggregate was replaced with recycled asphalt pavement) and CS reinforcement. The composition of the concrete mixtures is shown in Table 2. The culvert was coated with plastic foil for 24 hours after pouring. The culvert runs parallel to the roadway and collects the waste waters that, during winter season, are contaminated by de-icing salts; in addition, it is unsheltered from the rain and exposed to wetting and drying cycles. The culvert has a slight slope that promotes the flow of water in direction *A*→*F*.

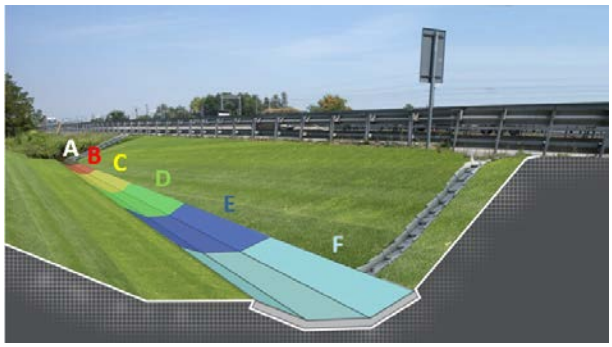

Fig. 1. Schematic of the division of the culvert into segments (courtesy of Pavimental)

Table 1. Combinations of reinforcement and concrete in the six segments of the RC culvert

Segment	Concrete	Reinforcement
A	Reference	Carbon steel (CS)
B	Seawater	Carbon steel (CS)
C	Seawater	Stainless steel 1.4311 (SS-304)
D	Seawater	Stainless steel 1.4362 (SS-23-04)
E	Seawater	GFRP
F	RAP	Carbon steel (CS)

2.1 Electrodes and probes

The evolution of the corrosion conditions of the reinforcements is monitored by means of various kinds of connections and probes that are embedded in the concrete. Two types of reference electrodes were used: a silver/silver chloride (SSC) commercial reference electrode (that was embedded next to all metallic reinforcements) and an activated titanium (Ti-Ref) electrode made of a thin wire taken from a cathodic protection mesh (this electrode was embedded also next to GFRP reinforcement). Both electrodes were fixed on one of the transverse bars of the reinforcement. In segment *B*, an activated titanium mesh was laid at the bottom of the slab, to allow linear polarisation measurements and for possible future application of cathodic protection.

Table 2. Composition of concrete mixtures, in kg/m^3 (from Buzzi)

Concrete	Reference	Seawater	RAP
Cement CEM II/A-LL 42.5R	335	335	335
Fly ash	30	30	30
Sand 0-5 mm	800	800	766
Gravel 5-7 mm	365	365	246
Gravel 8-15 mm	630	630	526
RAP	-	-	226
Superplasticiser	2.19	2.19	2.19
Retarding agent	-	0.76	-
Water	175	-	175
Seawater	-	175	-
w/c ratio	0.52	0.52	0.52

Specific “multi-reinforcement” and resistivity probes were designed and assembled in the laboratory. Multi-reinforcement probe contains segments of CS, SS-304 and SS-23-04 and it was embedded in segments *A*, *B* and *F*, so as to allow those combinations of type of rebar and type of concrete that could not be performed on real scale; resistivity probe consists of two parallel activated titanium wires (length and distance of 10 mm) and it was embedded in all segments. All probes were fixed to the reinforcing mesh and hence they have the same nominal concrete cover (Fig. 2).

The electrical connections to reinforcements, probes and electrodes were collected in an accessible electric cabinet located next to the culvert and they were carefully checked before concrete pouring.

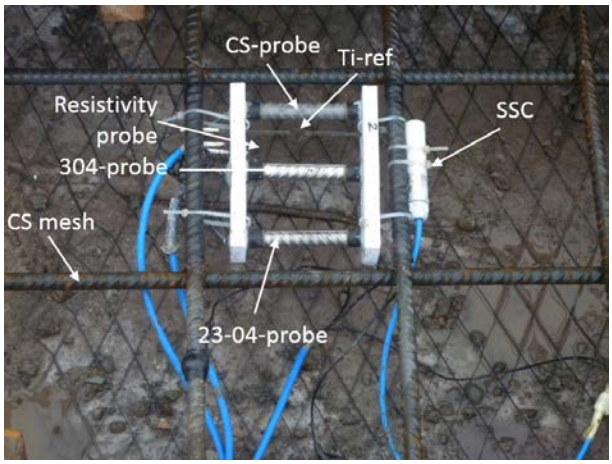

Fig. 2. CS mesh, multi-reinforcement probe, reference electrodes and resistivity probe in segment *B* before pouring (activated titanium mesh is also visible at the bottom)

2.2 Initial analyses

During pouring, four cubes with size 150 mm were taken from each concrete batch. Two cubes were brought to the laboratory to measure the compressive strength after 28 days of wet curing at about 95% RH (during curing the electrical resistivity was also measured) and the initial chloride content (by means of potentiometric titration). Two cubes were left in the culvert for future measurements (Fig. 3).

Fig. 3. View of the culvert

2.3 Monitoring of corrosion conditions

The potential of metallic reinforcement and all embedded probes and the electrical resistivity of concrete were regularly measured, roughly once a month. The potential was also measured versus an external copper/copper sulphate electrode (CSE). Besides those manual measurements, since June 2017 the potential of the reinforcement was also monitored with a data acquisition system, with frequency of one measurement every hour.

For GFRP reinforcement, specific monitoring techniques are under investigation (Khatibmasjedi and Nanni, 2017).

2.4 Inspection after 1 year

In October 2017, after almost a year since the construction, a detailed inspection was carried out that included potential mapping for all segments except *E* and linear polarisation measure for segment *B*. Several concrete cores with diameter of 50 mm were taken from the culvert: one core from the slab in each segment and three cores from the eastern lateral wall, two under the water discharges (LE-1 and LE-3) and one in intermediate position (LE-2). They were subjected to laboratory tests to determine chloride profiles on slices with thickness of 4 mm cut with a 1-mm thick saw. The carbonation depth was checked by means of spraying phenolphthalein indicator on the holes of the cores and it was nil in all cases.

3.0 RESULTS AND DISCUSSION

3.1 Initial characterisation of concrete

Fig. 4 shows the evolution of the electrical resistivity of concrete measured on the cubes during wet curing: all concretes showed an increasing trend, up to values of about 50 Ω·m for *reference* and *seawater* concretes and 70 Ω·m for *RAP* concrete. The average compressive strength at 28 days was 33 MPa for *reference* concrete, 42 MPa for *seawater* concrete and 32 MPa for *RAP* concrete; densities were 2280 kg/m^3, 2307 kg/m^3 and 2300 kg/m^3, respectively. The initial chloride content was negligible (0.01 %) in *reference* and *RAP* concretes and 0.11 % in *seawater* concrete (all percentages are referred to concrete mass). The latter value is slightly lower than the theoretical chloride content in *seawater* concrete that is 0.16 %. The initial chloride content of RAP aggregate could not be measured, however from leaching tests it was estimated to be lower than 0.01%

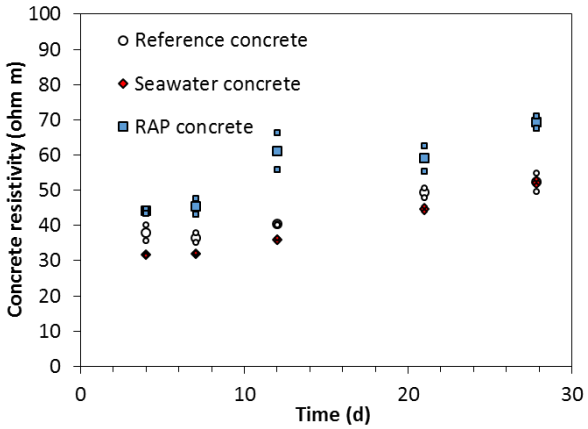

Fig. 4. Electrical resistivity of concrete cubes during wet curing (larger symbols indicate average values)

3.2 Evolution of corrosion parameters

Figure 5 shows the corrosion potential of CS reinforcement measured versus the SSC reference electrode in segments *A*, *B* and *F*: initially, in the first hours after pouring, all potentials were quite low, more negative than -700 mV vs SSC, then they progressively increased – with different rates – and

reached values between -100 and -300 mV vs SSC. The initial increase can be attributed to the passivation of CS, while the subsequent variations are more likely due to environmental variations of temperature and humidity. After about a year, the potential was around -150 mV vs SSC in *reference* and *RAP* concretes and -275 mV vs SSC in *seawater* concrete. Considering CS in *seawater* concrete, similar values of potential were obtained on laboratory specimens in conditions of exposure outdoor unsheltered, and corrosion rate measurements indicated that CS was mainly passive (Lollini *et al.*, 2017).

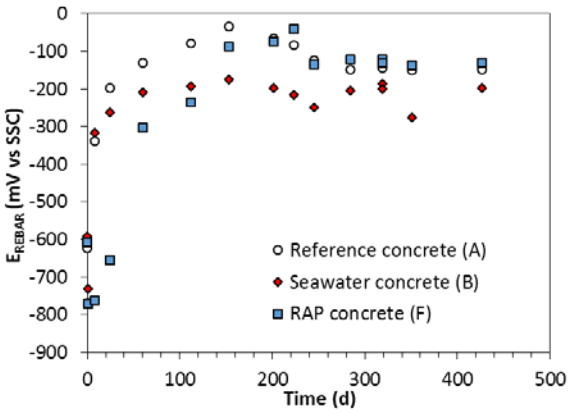

Fig. 5. Corrosion potential of carbon steel reinforcement measured versus the embedded SSC reference electrode in segments *A*, *B* and *F*

Figure 6 shows the corrosion potential of SS-304 and SS-23-04 in *seawater* concrete (segments *C* and *D*, respectively): the initial values were about -400 mV vs SSC for SS-304 and -300 mV vs SSC for SS-23-04, and also in these cases they progressively increased and reached values between 0 and -100 mV vs SSC. Overall the potential of SS-304 was 50 mV lower than that of SS-23-04; this behaviour was also observed on laboratory specimens (Bertolini and Gastaldi, 2011).

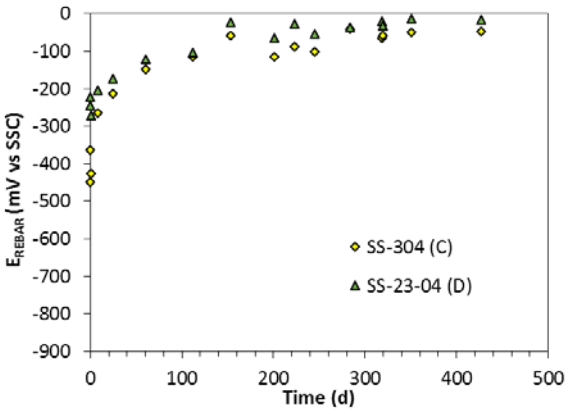

Fig. 6. Corrosion potential of austenitic (SS-304) and duplex (SS-23-04) stainless steel reinforcement measured versus the embedded SSC reference electrode in *seawater* concrete

Figs. 7-9 show the corrosion potential of carbon steel, austenitic (SS-304) and duplex (SS-23-04) stainless steel bars of the multi-reinforcement probes embedded in three segments (*A*, *B* and *F*) that are representative of the three types of concrete. For carbon steel (Fig. 7) the trend is very similar to that in Fig. 5, that was obtained on the reinforcement mesh, although all values are slightly higher. This shift towards more positive values may be due to the fact that, unlike the reinforcing mesh (that was used "as received" on site), the multi-reinforcement probes were prepared in the laboratory and the CS bars were cleaned by sandblasting and degreasing.

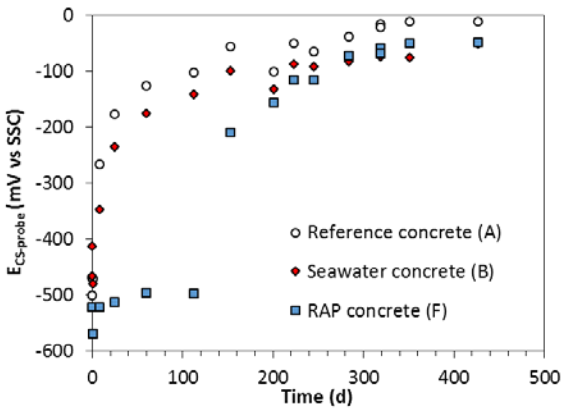

Fig. 7. Corrosion potential of carbon steel bar of the multi-reinforcement probes embedded in segments *A*, *B* and *F*

Stainless steel 304 probe (Fig. 8) seems to have experienced some problems with connection in segments *B* and *F*, probably due to pouring and compaction, while in segment *A* the potential after a year was about -50 mV vs SSC. Since this potential is very close to that obtained on the mesh in *seawater* concrete (Fig. 6), it is reasonable to assume that the corrosion behaviour is similar, and this is a further confirmation of the passive behaviour of stainless steel 304 in *seawater* concrete.

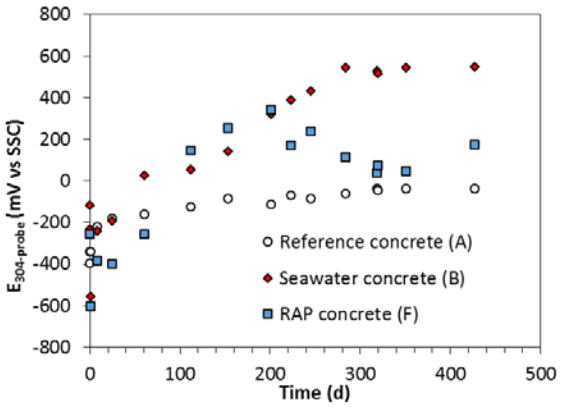

Fig. 8. Corrosion potential of austenitic (SS-304) stainless steel bar of the multi-reinforcement probes embedded in segments *A*, *B* and *F*

Even duplex stainless steel 23-04 probe (Fig. 9) showed – in all segments – values that are very similar to those measured on the mesh in *seawater* concrete (Fig. 6).

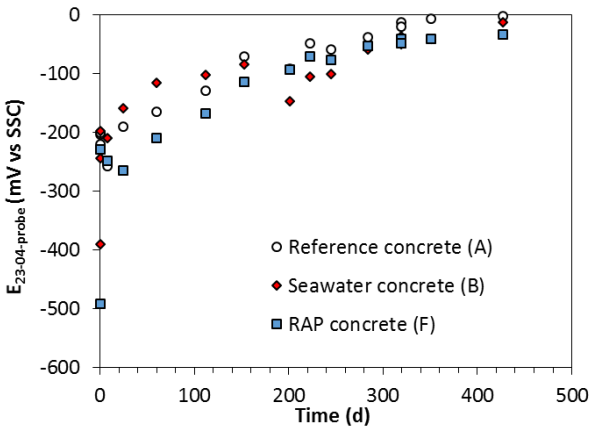

Fig. 9. Corrosion potential of duplex (SS-23-04) stainless steel bar of the multi-reinforcement probes embedded in segments *A*, *B* and *F*

The potential of the metallic reinforcing meshes was also monitored with a data logger: Fig. 10 shows, as an example, the potential of the reinforcing meshes of the two grades of stainless steel in *seawater* concrete measured versus embedded SSC electrode in June 2017. The higher frequency of detection allowed highlighting daily potential variations of the order of 50 mV, with lower values during day and higher values during night. Similar oscillations were observed on segments *A*, *B* and *F*. Besides those measurements that were mainly aimed at checking the data logger system, the data logger will be essential after the end of the project to allow long-term monitoring of the future corrosion conditions minimising the inspections and manual measurements.

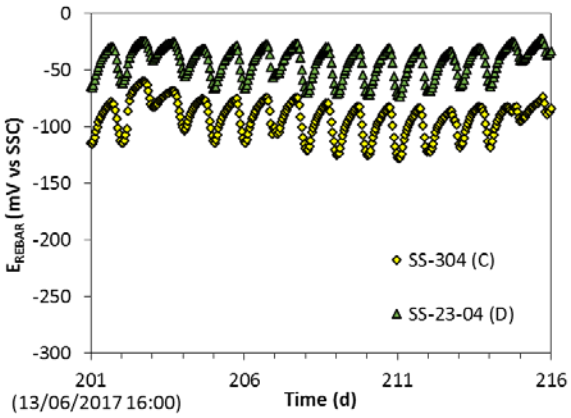

Fig. 10. Corrosion potential of austenitic (SS-304) and duplex (SS-23-04) stainless steel reinforcement measured versus the embedded SSC reference electrode in segments *C* and *D*, respectively

In segment *B*, the presence of the activated titanium mesh allowed to perform linear polarisation measurements to estimate the corrosion rate of the reinforcement mesh, as well as of each bar of the multi-reinforcement probe. These measurements were carried out during the detailed inspection in October 2017, both in normal exposure conditions and after thorough wetting of the slab with freshwater for 4 hours and the results are reported in Table 3. The corrosion rate of the reinforcing CS mesh was around 1 mA/m^2, indicating almost negligible corrosion, and it slightly increased after wetting, yet it remained negligible. The carbon steel probe showed even lower values (0.4 mA/m^2), probably due to the previously mentioned initial surface condition. The austenitic stainless steel probe showed very small values (<0.1 mA/m^2), while duplex stainless steel probe showed values around 3 mA/m^2, even higher than carbon steel. This increased corrosion rate of such grade of stainless steel has also been observed in the laboratory and should not be considered indicative of a corrosion activity, but rather to superficial conditions of the bar (Gastaldi and Bertolini, 2014; Lollini *et al.*, 2018).

Table 3. Results of linear polarisation measurements in segment *B* (*seawater* concrete)

Electrode	v_{CORR} (mA/m^2)	$v_{CORR,wet}$ (mA/m^2)
Carbon steel mesh	0.94	1.24
CS-probe	0.45	0.43
304-probe	0.04	0.01
23-04-probe	3.03	3.44

Figure 11 shows the electrical resistivity of concrete that was measured with the probe embedded in the concrete at the depth of the reinforcement. Initial values were very low (1-2 Ω·m) for all segments, then in the first couple of months they increased reaching values around 20 Ω·m. After this, greater variations occurred. Overall, initially chloride-free concrete (i.e. *reference* and *RAP* concrete of segments *A* and *F*, respectively) showed the lowest values (e.g. about 40 Ω·m after a year), while *seawater* concrete (segments *B*-*E*) showed the highest values (e.g. 75-100 Ω·m after a year).

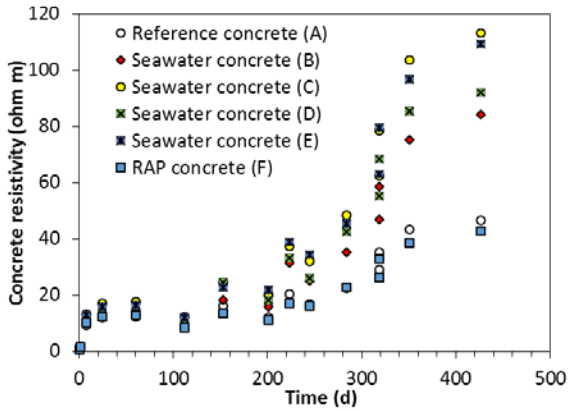

Fig. 11. Electrical resistivity of concrete measured with the embedded resistivity probe at the depth of the reinforcement

These results are not consistent with those obtained on the cubes (Fig. 4), where *seawater* concrete showed similar or lower values with respect to *reference* concrete, as expected due to the presence of chlorides (Saleem at al., 1996). Nevertheless, the monitoring of the resistivity with embedded probes is expected to highlight possible future variations in the conditions of the concrete at the depth of the reinforcement, in terms of chloride and humidity content.

All the electrochemical measurements that are performed by means of the embedded electrodes and probes are representative of the corrosion conditions of steel in a relatively small area localised in the vicinity of the electrodes themselves. Potential mapping, on the other hand, allows highlighting differences in the corrosion behaviour over the surface of the slab. Figs. 12 and 13 show, as an example, the potential mappings that were obtained on carbon steel reinforcement in segments *A* and *B*, respectively. The potential differences between different parts of the reinforcement were relatively small, lower than 100 mV. No substantial potential gradients occurred, so it can be concluded that in each segment the corrosion condition of the reinforcement is still uniform over the whole surface of the slab.

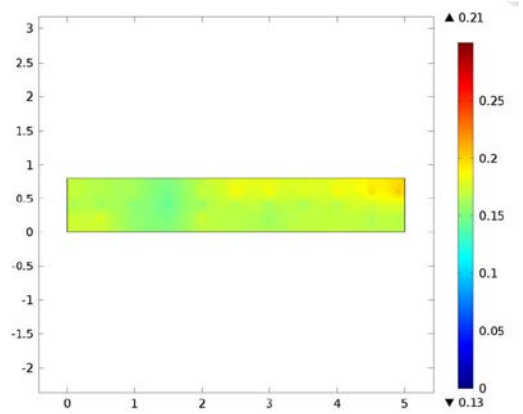

Fig. 12. Potential mapping of carbon steel reinforcement in segment *A* (values in -V vs CSE)

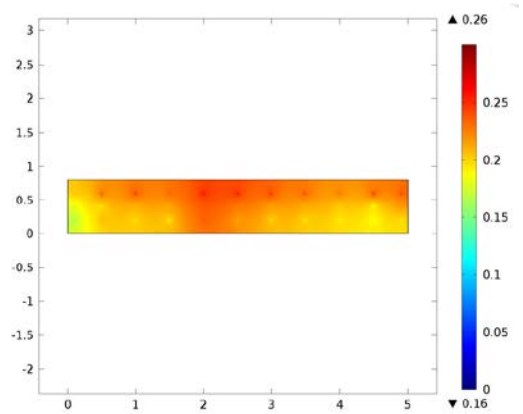

Fig. 13. Potential mapping of carbon steel reinforcement in segment *B* (values in -V vs CSE)

3.3 Chloride profiles

Figures 14 and 15 show the chloride profiles obtained on the cores after 1 year of exposure. Cores taken from concretes that were initially chloride-free (i.e., *reference* concrete of segment *A*, *RAP* concrete of segment *F* and concrete of the lateral walls *LE*) showed an almost flat profile, with chloride amounts close to the initial value, as it can be seen in Fig. 14. *RAP* concrete had a slightly higher chloride content, probably due to the presence of small amounts of chlorides in the RAP aggregate, that diffused inside the cement paste. Anyway, the profile was flat and the chloride contents were negligible. As expected, no substantial chloride penetration occurred during the first year of exposure.

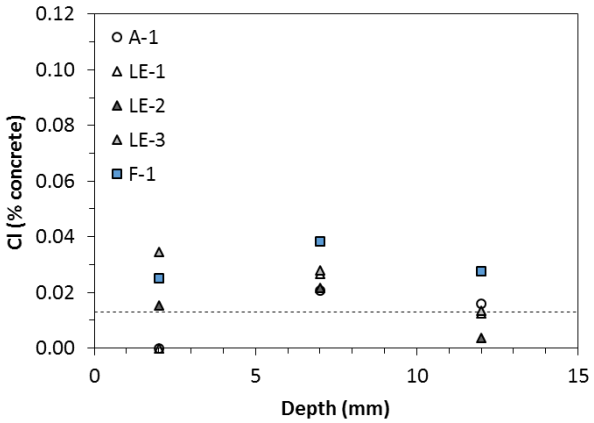

Fig. 14. Chloride profiles in segments *A* and *F* and lateral walls *LE* (dotted line indicates initial chloride content measured in concrete *A*)

In cores taken from *seawater* concrete, the chloride content in the first layer was lower than the initial value, then the content increased up to the initial value (Fig. 15). This reversed shape of the profile was observed on all segments, and it indicates that not only chloride penetration did not take place, but even chloride leaching may have occurred close to the surface. Chloride leaching can be attributed to wetting with rain water or freshwater, even in the early stages after pouring. It should be mentioned that the whole slab was often wetted with freshwater during inspection.

Given the obtained chloride profiles, and considering that the nominal concrete cover is 30 mm, the chloride content at the depth of the reinforcement is the same as the initial one.

3.4 Corrosion conditions

Table 4 summarises the corrosion-related parameters for metallic reinforcements after almost a year of exposure. The chloride contents are expresses with respect to cement weight. For CS reinforcements embedded in *reference* and *RAP* concretes, the high potentials indicate that the rebars are in conditions of passivity. This result

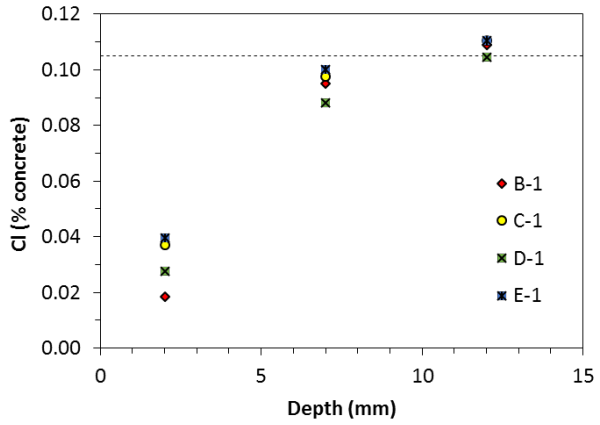

Fig. 15. Chloride profiles in segments *B-E* (dotted line indicates initial chloride content measured in *seawater* concrete)

matches the expectations, since no chloride penetration occurred and the chloride content at the depth of the reinforcement was around 0.1-0.2% with respect to cement weight, well lower than the critical threshold usually considered for CS in concrete that is around 0.4-1% (Bertolini *et al.*, 2013). In *seawater* concrete the corrosion conditions of CS were less clear, with lower potential values, yet almost negligible corrosion rate and intermediate chloride content (0.75% with respect to cement weight). The two grades of stainless steel (SS-304 and SS-23-04) embedded in *seawater* concrete, given the very high values of potential and a chloride content lower than the critical chloride threshold of these steels (around 8 and 3%, respectively (Gastaldi and Bertolini, 2014)), can be considered in passive conditions. Of course, the evolution of the corrosion parameters of the various reinforcements will be monitored to highlight the effect of environmental actions and chloride penetration on the corrosion conditions.

Table 4. Summary of corrosion potential, corrosion rate, concrete resistivity and chloride content at the depth of the reinforcement after almost a year of exposure

Segment	E_{REBAR} (mV vs SSC)	v_{CORR} (mA/m^2)	Resistivity (Ω·m)	Chlorides (% vs cem)
A	-151	-	43	0.1
B	-275	0.94	75	0.75
C	-49	-	104	0.75
D	-14	-	85	0.75
F	-136	-	39	0.2

4.0 CONCLUSIONS

The corrosion conditions of various types of reinforcements embedded in *reference*, *seawater* and *RAP* concretes in real-scale and exposure conditions were investigated by monitoring corrosion parameters and analysing concrete specimens.

After a year of exposure, no chloride penetration occurred and the chloride content at the depth of the reinforcement was the same as the initial content.

Carbon steel reinforcement in both *reference* and *RAP* concretes was characterised by relatively high potentials that, together with the low chloride content, indicate conditions of passivity. In *seawater* concrete the corrosion conditions of carbon steel were uncertain, given the intermediate values of potential and chloride content and the negligible values of corrosion rate.

Stainless steel reinforcement of austenitic (SS-304) and duplex (SS-23-04) grades were characterised by high values of potentials that were indicative of passivity, in agreement with the high critical chloride threshold contents of such steels, much higher than the chloride content resulting from seawater.

Acknowledgements

The support of Infravation (GA No. 31109806.005-SEACON) is gratefully acknowledged. The Authors wish to thank all the partners of the project, in particular University of Miami (leader), Buzzi (for characterising and supplying concrete mixes and taking concrete cores), Pavimental (for making the site available and taking care of all aspects related with design and construction), Acciaierie Valbruna (for supplying stainless steel bars) and ATP (for supplying GFRP bars).

References

Bertolini, L., Elsener, B., Pedeferri, P., Redaelli, E., Polder, R., 2013. Corrosion of steel in concrete: prevention, diagnosis, repair, 2nd edition, Wiley-VCH.

Bertolini, L., Gastaldi, M., 2011. Corrosion resistance of low-nickel duplex stainless steel rebars. Materials and Corrosion, 62:120-129.

Gastaldi, M., Bertolini, L., 2014. Effect of temperature on the corrosion behaviour of low-nickel duplex stainless steel bars in concrete. Cement and Concrete Research, 56:52-60.

Khatibmasjedi, M., Nanni, A., 2017. Durability of GFRP reinforcement in seawater concrete – Part I. American Concrete Institute Special Publication.

Lollini, F., Carsana, M., Gastaldi, M., Redaelli, E., Bertolini, L., Nanni, A., 2016a. Can seawater be used as mixing water for durable and sustainable RC structures?, NACE International - Concrete Service Life Extension Conference, Orlando (FL), USA, p. 1-9.

Lollini, F., Carsana, M., Gastaldi, M., Redaelli, E., Bertolini, L., Nanni, A., 2016b. Preliminary assessment of durability of sustainable RC structures with mixed-in seawater and stainless steel reinforcement. Key Engineering Materials, 711:52-59.

Lollini, F., Carsana, M., Gastaldi, M., Redaelli, E., Torabian Isfahani, F., Bertolini, L., 2017. Corrosion behaviour of reinforcement in concrete with chloride-contaminated raw materials-Part I: Laboratory tests [Comportamento alla corrosione di armature in calcestruzzo con materie prime contaminate da cloruri - Parte I: prove di laboratorio]. Metallurgia Italiana, 109(7-8):39-42.

Lollini, F., Carsana, M., Gastaldi, M., Redaelli, E., 2018. A review on corrosion behaviour of stainless steel reinforcement in concrete. Accepted for publication in Corrosion Reviews.

Redaelli, E., Carsana, M., Gastaldi, M., Lollini, F., Torabian Isfahani, F., Bertolini, L., 2017. Corrosion behaviour of reinforcement in concrete with chloride-contaminated raw materials-Part II: On site preliminary results [Comportamento alla corrosione di armature in calcestruzzo con materie prime contaminate da cloruri - Parte II: risultati preliminari di prove in campo]. Metallurgia Italiana, 109(7-8):43-46.

Saleem, M., Shameem, M., Hussain, S.E., Maslehuddin, M., 1996. Effect of moisture, chloride and sulphate contamination on the electrical resistivity of Portland cement concrete. Construction and Building Materials, 10(3):209-214
.